A Bombyx homolog of ovo is a segmentation gene that acts downstream of Bm-wnt1 (Bombyx wnt1 homolog)

A Bombyx homolog of ovo is a segmentation gene that acts downstream of Bm-wnt1(Bombyx wnt1 homolog)

Hajime Nakao
Insect Genome Research and Engineering Unit, Division of Applied Genetics, Institute of Agrobiological Sciences, National Agriculture and Food Research Organization (NARO), 1-2 Oowashi, Tsukuba, Ibaraki 305-8634, Japan

Correspondence to Hajime Nakao
Insect Genome Research and Engineering Unit, Division of Applied Genetics, Institute of Agrobiological Sciences, National Agriculture and Food Research Organization (NARO), 1-2 Oowashi, Tsukuba, Ibaraki 305-8634, Japan
Tel.: +81-29-838-6127, Fax: +81-29-838-6028, E-mail: nakaoh@ affrc.go.jp

Keywords
Bombyx, ovo, wnt1, RNAi, segmentation, pair-rule genes

Abstract

Insect embryogenesis is divided into long and short/intermediate germ types. The long germ type may exhibit *Drosophila*-like hierarchical segmentation mechanisms, whereas the short/intermediate type assumes some repeating mechanisms that are considered to be ancestral. Embryogenesis in *Bombyx mori* possesses both characteristics. Here, *Bombyx ovo* homolog (*Bm-ovo*) was identified as a gene involved in segmentation. *ovo* is a *Drosophila* gene that encodes a zinc finger transcription factor and studies on its homolog functions in other systems have suggested that it acts as a switch to enable the initiation of differentiation from a progenitor cell state. This is the first description for *ovo* homologs being involved in insect segmentation. *Bm-ovo* is expressed dynamically during embryogenesis in a pattern that resembles that of gap and pair-rule genes. In *Bm-ovo* RNAi knockdown embryos, posterior segmentation does not proceed. In addition, defects in anterior segments are observed. In *Bm-wnt1* knockdown embryos, the *Bm-ovo* expression pattern was changed, suggesting that *Bm-wnt1* is an upstream regulator of *Bm-ovo*. The involvement of *Bm-ovo* may represent a novel ancestral step under the control of *wnt* genes in insect segmentation: this step may resemble those operating in cell differentiation processes.

Introduction

In insect embryos, maternal, gap, and pair-rule genes are successively expressed to produce segments along the anterior-posterior (AP) axis. Maternal genes dictate the AP axis. Gap genes subdivide embryos into broad domains according to their expression profiles. The expression of seven to eight stripes of pair-rule genes serves as a template for future segments. Insect embryogenesis has been largely categorized into long and intermediate/short germ types (Davis and Patel, 2002; Liu and Kaufman, 2005; Peel et al., 2005). In the long germ type, as represented by *Drosophila*, the combinatorial input of maternal and gap genes directs the expression of the individual stripes of pair-rule genes, which leads to the nearly simultaneous expression of pair-rule stripes, i.e., segment formation (Pankratz and Jäckle, 1993). In contrast, in the short/intermediate type, posterior segments are sequentially added, in which some repeating segmentation mechanisms are likely to operate. In the short germ-type insect *Tribolium*, the wave-like expression of pair-rule genes *even-skipped* (*eve*) and *odd-skipped* (*odd*) has been observed in the pre-segmental area (Sarrazin et al., 2012; El-Sherif et al., 2012). The pair-rule genes, *eve*, *odd*, and *runt* (*run*) interact positively and negatively to form a circuit that appears to be responsible for the striped expression of these genes. Thus, the wave-like expression of a subset of pair-rule genes may be passed onto the pair-rule gene circuit, leading to the production of segments (pair-rule gene stripes) in a clock-like manner (Choe et al., 2006; Lynch et al., 2012).

It is commonly acknowledged that the latter *Tribolium*-like segmentation mode is ancestral, while the former *Drosophila*-like hierarchical segmentation mode is derived. Recent evidence suggests that both modes may operate in some species (Rosenberg et al., 2014), such as *Bombyx mori*.

B. mori is a lepidopteran insect, the segmentation mechanisms of which have remained elusive. Its embryogenesis has long and short/intermediate-like features. The egg has a large embryonic primordium, within which individual segments are fate mapped without a growth zone early in embryogenesis similar to long germ insects (Myohara, 1994). However, when pair-rule gene interactions were examined, *B. mori* exhibited *Drosophila*- and *Tribolium*-like characteristics (Nakao, 2015). Furthermore, the roles of *Bombyx wnt1*/*wingless* and the *Krüppel* homolog resemble those in short/intermediate insects: embryos show truncated phenotypes in the posterior region when these gene

(family) activities are perturbed (Beermann et al., 2011; Bolognesi et al., 2008, 2009; Miyawaki et al., 2004; Nakao, 2010, 2015; Yamaguchi et al., 2011; Cerny et al., 2005; Liu and Kaufman, 2004; Mito et al., 2006). Embryonic *Bm-wnt1* is considered to have two functions: its organizing function in posterior development, as reflected in the knockdown phenotype as described above, and its function as a segment polarity gene, similar to that in *Drosophila*. During normal embryogenesis, *Bm-wnt1* is expressed in the large posterior domain in the early stages, the expression domain then recedes posteriorly, and segmental stripes begin to appear in an anterior to posterior sequence (Nakao, 2010). Posterior expression appears to be responsible for posterior organization functions, while segmental expression appears to exhibit a segment polarity function that has not yet been experimentally validated in *Bombyx*. Furthermore, the addition of supernumerary posterior segments is induced at the posterior terminus in a manner that resembles that of short/intermediate insects by the knockdown of the *hunchback* homolog (*Bm-hb*) (Nakao, 2016). These findings strongly suggest that the short/intermediate type mode of segmentation is operating in normal *Bombyx* embryogenesis.

An *ovo* homolog from *B. mori* (*Bm-ovo*) was described herein. *ovo* is a *Drosophila* gene that encodes an evolutionarily conserved zinc finger transcription factor with various biological functions. It is required in the female germ line for proper oogenesis: the mutants display egg chambers filled with excess undifferentiated germ cells, an ovarian tumor phenotype (Oliver, 1987). *ovo* is also involved in early germ line development: the transcript is deposited in the germ plasm as a maternal factor, regulating the expression of *vasa* (Yatsu et al., 2008). In the zygote, often referred to as *shavenbaby* (*svb*) at this stage, it is necessary and sufficient to cell-autonomously direct the formation of denticles (trichome-cytoplasmic extrusion of epidermal cells) in the ventral epidermis of the embryo abdomen, in which there is a segmentally repeating denticle pattern separated by naked cuticle, thereby contributing to the binary choice to produce either a naked cuticle or denticles. The upstream regulation of *svb* has been investigated. The high mobility group (HMG)-domain protein SoxNeuro (SoxN) is necessary and sufficient to cell-autonomously direct the expression of *svb*. SoxN, in turn, receives positive and negative inputs from the epidermal growth factor receptor (Egfr) ligand Spitz (Spi) and Wingless (Wg), respectively. These mechanisms result in the restriction of trichome-producing cells. The closely related protein of Spi, Dichaete is co-regulated

with Spi and has a partially redundant function in the activation of *svb*, albeit to a lesser extent. However, these regulatory relationships are not strictly hierarchical, but complex feedback mechanisms are involved (Overton et al., 2007).

Apart from *Drosophila*, *ovo* homologs are isolated from diverse animals. The mouse homolog also controls germline and epidermis differentiation. In *C. elegans*, the *ovo* homolog *lin-48* is required for the development of hindgut. These findings point to the role of *ovo* homologs in the differentiation and maintenance of specific cell types (Wieschaus, 1984; Oliver, 1987; Dai, 1998; Johnson, 2001). More recently, human homolog of *ovo* (*OVOL1*) was shown to regulate the transition of progenitor to differentiated trophoblast cells (Renaud et al., 2015).

In the present study, the embryonic functions of *Bm-ovo* were examined. *Bm-ovo* expression during the embryonic stage resembled that of gap and pair-rule genes. Embryonic *Bm-ovo* RNAi embryos showed segmentation defects in the gnathal/thoracic region and posterior abdomen. In the posterior body part, the abnormal expression of some pair-rule genes that are crucial for establishing pair-rule gene expression patterns was observed: the posterior part did not produce pair-rule stripes, but a broad band of expression was observed in the affected region for the pair-rule genes examined. In *Bm-wnt1* knockdown embryos, alternation in *Bm-ovo* expression pattern was observed, suggesting that *Bm-wnt1* is an upstream regulator of *Bm-ovo*. This interaction may be related to those operating in *Drosophila* embryonic epidermal patterning as described above.

The involvement of *Bm-ovo* may represent a novel ancestral step under the control of *wnt* genes in insect segmentation, and this step may resemble those operating in cell differentiation processes.

Materials and Methods

Silkworm strains, rearing, and development

The *B. mori* strain *pnd-2* was used in this study. Silkworms were reared on an artificial diet (Nippon Nosanko). Refer to Nagy et al. (1994) for a general description of early *Bombyx* development.

Identification and isolation of Bm-ovo cDNA

The *Drosophila ovo* sequence was used to search the *Bombyx* cDNA database (Mita et al., 2003) for *Bombyx ovo* homologs and one wing-disk-derived cDNA was identified. cDNA was obtained and initial analyses were performed using this cDNA. The annotated genome database (KAIKObase; Mita et al., 2004) subsequently became available, which revealed that the open reading frame of *Bm-ovo* comprises four exons (E1, E2, E3 and E4; gene ID: BMgn000987). The cDNA clone described above was found to lack the second exon. To obtain cDNA species expressed during early embryogenesis, a PCR amplification procedure was employed. Total RNAs in embryos 14 and 20 hours AEL were prepared using TRIZOL reagent (Invitrogen). Single-strand cDNAs were synthesized using total RNAs as templates by PrimeScript^{TM}II 1st strand cDNA Synthesis Kit (TAKARA) according to the manufacturer's instructions. With these cDNAs, PCR amplification was performed using PrimeSTAR GXL DNA Polymerase (TAKARA). A primer pair was set at the sequence near the start and stop codons, respectively, so as to amplify the full open reading frame. PCR conditions were 40 cycles at 98°C for 10 s; at 55°C for 15 s; at 68°C for 3 min. The primer pair was the *Bm-ovoCp*, 5'-primer and *Bm-ovoE3-4p*, 3'-primer (see below). The amplified product was analyzed using 1% agarose gel electrophoresis. The results obtained revealed the predominant amplification of an approximately 2.6-kbp product from both templates (Supplementary Fig. 1). The amplified product was cloned and sequenced. The sequence analysis revealed that it had all four exons. Subsequent analyses were performed using this cDNA.

In situ hybridization

Fixation and *in situ* hybridization were performed as previously described (Nakao, 1999, 2010). Probes for *Bm-eve* and *Bm-wnt1* were previously described (Nakao, 2010). Probes for *Bm-ovo*, designated as *Bm-ovoCp*, *Bm-ovoE1p*, *Bm-ovoE2p* and *Bm-ovoE3-4p*, were synthesized using cloned cDNAs. cDNAs were PCR fragments amplified using the primers described below. The primer pairs used for the amplification of these fragments were as follows: *Bm-ovoCp*, 5'-primer: 5'-GGGGGATCCAGTCCTAACGAAGCGGCCAA-3', 3'-primer: 5'-

CCCAAGCTTTTTATACGGTCTGACTCCGG-3'; *Bm-ovoE1p*, 5'-primer: 5'-GGGGGATCCAGTCCTAACGAAGCGGCCAA -3', 3'-primer 5'-CCCAAGCTTCAGTGCATTCCTTTTCTTTATCC -3'; *Bm-ovoE2p*, 5'-primer: 5'-GGGGGATCCCGCACAAAAGAAACTAGACG -3', 3'-primer 5'-CCCAAGCTTAGCACTAAAACAGGTCGTGC -3'; *Bm-ovoE3-4p*, 5'-primer: 5'-GGGGGATCCTAGGACTACCAGCAGAGCTT -3', 3'-primer 5'-CCCAAGCTTAATTGTGTACTGGCATGGGC -3'. The *Bm-ovoCp* primer pair was used for amplification from the cloned cDNA template (fufe-P20_F_P18), and the amplified product comprised approximately 0.3-kb exon 1 and 0.3-kb exon 3 (see the **Results** section). *Bm-ovoE1p*, *E2p* and *E3-4p* primer pairs were used for amplification from the cDNA prepared using PrimeScript™ II 1st strand cDNA Synthesis Kit (TAKARA) and total RNA at 20 hours AEL. The amplified products were approximately 0.3, 0.5, and 0.6 kbp, which corresponded to parts of exons 1, 2, and 3-4, respectively. After amplification, cDNAs were cloned into pBluescript vectors. In order to obtain probes, plasmid DNA was cut with an appropriate enzyme and RNA probes were synthesized using either T3 or T7 polymerase, depending on the direction of the insert using DIG RNA Labeling Kit (SP6/T7) (Roche).

RNAi

The RNAi procedure was described previously (Nakao, 2012). The templates used for *in vitro* transcription were PCR fragments of the corresponding genes, flanked by T7 promoter sequences. Regarding *Bm-ovo* RNAi, three different dsRNAs, designated as *Bm-ovoCRNAi*, *Bm-ovoE1RNAi* and *Bm-ovoE3-4RNAi*, were used in analyses. The primer pairs used for amplification were as follows: *Bm-ovoCRNAi*, 5'-TAATACGACTCACTATAGGGAGAAGTCCTAACGAAGCGGCCAA-3', 5'-TAATACGACTCACTATAGGGAGATTTATACGGTCTGACTCCGG-3'; *Bm-ovoE1RNAi*, 5'-TAATACGACTCACTATAGGGAGAAGTCCTAACGAAGCGGCCAA-3', 5'-TAATACGACTCACTATAGGGAGACAGTGCATTCCTTTTCTTTATCC-3'; *Bm-ovoE3-4RNAi*, 5'-TAATACGACTCACTATAGGGAGATAGGACTACCAGCAGAGCTT-3', 5'-TAATACGACTCACTATAGGGAGAAATTGTGTACTGGCATGGGC. *Bm-ovoC*,

ovoE1, and *E3-4RNAi* targets corresponded to the regions amplified by the *Bm-ovoCp*, Bm-*ovoE1p*, and *Bm-E3-4p* primer pairs described above, respectively. For *Bm-wnt1* RNAi, two independent dsRNA corresponding to different part of the gene was used for the analysis. The primer pairs were as follows: *Bmwnt1RNAi1*, 5'-TAATACGACTCACTATAGGGAGAGCAGAATGAAGTGTCTGTGG-3', 5'-TAATACGACTCACTATAGGGAGAAAGCCGATGTTGTCGCTGCA-3', *Bmwnt1RNAi2*, 5'-TAATACGACTCACTATAGGGAGAAGGGAATTCGTTGATACCGG-3', 5'-TAATACGACTCACTATAGGGAGAACCTCGCAACACCAATGGAA-3'.

Results

Identification of a Bombyx ovo homolog

A recent study described the *ovo* homolog from *Bombyx* (*Bm-ovo*); multiple forms of spliced variants were differentially expressed among the tissues examined (Xue et al., 2014). The identification of *Bm-ovo* in the present study was performed independently in our laboratory. After cDNA database search (Mita et al., 2003), a cDNA derived from wing-disk-expressed mRNA was obtained (fufe-P20_F_P18). Initial analyses were performed using a probe (*Bm-ovoCp*) or double-stranded RNA (*Bm-ovoCRNAi*) made from this cDNA as a template. However, a subsequent analysis revealed that this mRNA species lacked exon E2 and was poorly represented in early embryonic stages (see **Materials and Methods**). After obtaining embryonically expressed cDNA, which comprised exons E1, E2, E3 and E4, analyses were also performed using a few mutually independent probes or dsRNA in addition to the analyses described above. The results of these analyses were essentially the same.

Bm-ovo embryonic expression

A gene expression analysis of *Bm-ovo* was performed by *in situ* hybridization using the probes, *Bm-ovoCp*, *E1p*, *E2p* and *E3-4p* (see **Materials and Methods**). Irrespective of probes used, the results were essentially the same (Supplementary Fig. 2). Just after egg laying, weak expression was observed in the germ anlage, suggesting its maternal load

(Fig. 1A, B). Regional heterogeneities in expression were not detected within the germ anlage, suggesting that the transcript did not accumulate in the putative germ plasm, although the existence of germ plasm was suggested by *Bm-nanosO* (*Bombyx nanosO*) expression pattern (Nakao et al., 2008). Specific accumulation in the germ line was not observed during the time period examined in the present study, i.e., up to 5 days AEL (After Egg Laying), which was in contrast with previous findings obtained using *Drosophila* (Yatsu et al., 2008). Expression was dynamic more than 22 hours AEL and resembled that of the gap and pair-rule genes. At 22 hours, expression was detected in one anterior domain (head) and one large posterior domain (Fig. 1C). Later, the posterior domain resolved into three strong stripes (bands) and two weak stripes (bracketed) (Fig. 1D, E). The three strongly expressed stripes remained thereafter, and overlapped with *Bm-eve* stripes #2, #6, and #8 (Fig. 1F, G). Although it could not be determined due to technical difficulties which pair-rule stripes the weak *Bm-ovo* stripes corresponded to or which pair-rule stripes the broad strong *Bm-ovo* stripes exactly cover, a (morphological) comparison of single- and double-stained embryos suggested that stripes #1, #3, and #7 escaped *Bm-ovo* coverage at the later stages. However, the expression pattern of *Bm-ovo* suggested that the *Bm-ovo* posterior expression domain covered all the *Bm-ovo* stripes at least once, except for stripe #1. As the development proceeded, the background signal intensity transiently increased, region-specific staining became obscured (Fig. 1H), and background staining then decreased again (Fig. 1I).

Analysis of Bm-ovo functions using embryonic RNAi

Embryonic RNAi was used to analyze *Bm-ovo* functions. dsRNAs were injected into embryos at 0~2 hours AEL. As described above, three dsRNAs were used to examine phenotypes. Target gene expression was markedly reduced for all the dsRNAs used, suggesting that the RNAi procedure was effective (Supplementary Fig. 3).

The phenotypes of knockdown embryos were examined for their morphologies at 72 hour AEL. In RNAi-treated embryos, anomalies were observed in the anterior and posterior of embryos (Fig. 2). Anterior phenotypes represented defects in the morphology of the region encompassing gnathal/thoracic segments, with the mesothoracic segment being the most frequently affected. In these regions, the observed

phenotypes included irregular morphologies or the deletion of segments and/or appendages, or fused or disorganized gnathal/thoracic segments (Fig. 2B, C). In the posterior, the fusion of posterior abdominal segments was observed for all dsRNA species: in the most severe cases, a total of six abdominal segments were observed (Fig. 2B, C, Table 1). The identities of the remaining abdominal segments were not entirely clear. However, based on the observation that three proleg-bearing segments remained in RNAi treated embryos (Fig. 2B), the identities of A1 to A5 appeared to be preserved in the correct order (in the wild-type, prolegs were observed in A3-A6, also see below). In both phenotype classes, the severity of the phenotype appeared to differ between the dsRNAs used (Table 1); for example, the number of abdominal segments was significantly lower in *Bm-ovoE1RNAi* or *Bm-ovoE3RNAi* embryos than in *Bm-ovoCRNAi* embryos ($P<0.05$), reflecting the incomplete nature of the RNAi knockdown. Therefore, the knockout phenotype may differ from those observed here by the RNAi knockdown.

In order to elucidate the cause of these morphological consequences, embryos were analyzed molecularly. Since pair-rule genes were responsible for segment formation, the expression of three key pair-rule genes, *Bombyx even-skipped* (*Bm-eve*), *runt* (*Bm-run*), and *odd-skipped* (*Bm-odd*) was examined at 23~28 hours AEL when the full complement of each pair-rule gene stripe was expressed in wild-type embryos (Fig. 3A, C, E; Nakao, 2015). The most notable change was the broad expression of these pair-rule genes in the posterior region without the resolution of stripes after stripe #5, which is consistent with posterior abdominal segment fusion morphologies (*Bm-eve*, n=29/31; *Bm-run*, n=27/28; *Bm-odd*, n=50/54). In addition, the weak expression of the *Bm-eve* stripe #3 (and less frequently, stripe #2) was sometimes observed (n=15/21), together with the weak expression of *Bm-run* and *Bm-odd* stripe #2 (*Bm-run*, n=5/25; *Bm-odd*, n=16/51; Fig. 3B, D, F, Supplementary Fig. 4). However, it is important to note that although the intensity of expression was changed, patterning in the anterior region was essentially not affected by *Bm-ovo* RNAi, which is in contrast to posterior patterning in the affected embryos.

Bm-ovo is regulated by Bm-wnt1

The present findings show that *Bm-ovo* is involved in *Bombyx* body segmentation.

Bm-wnt1 also functions in the establishment of segments. These homologs are known to interact in *Drosophila* embryonic epidermal patterning as described in the **Introduction** section. Therefore, embryonic RNAi was used to test whether *Bm-ovo* and *Bm-wnt1* are interact and, if so, how. *Bm-ovo* RNAi was performed as described above and *Bm-wnt1* expression in the resulting embryos was compared with that in wild type embryos. As examined at ~23h AEL, *Bm-wnt1* expression in RNAi-treated embryos was similar to that in wild type embryos (n=14/14; Fig. 4A, B). However, at approximately 26h AEL, when more anterior segmental stripes of *Bm-wnt1* became visible, these stripe boundaries in treated embryos were more irregular, except for a few anterior-most stripes (n=20/20; black arrows in Fig. 4D), than those in wild type embryos, whereas differences were not observed in the posterior expression domain (n=34/34; white arrows in Fig. 4A-D). Next, *Bm-wnt1* RNAi was performed to examine changes in *Bm-ovo* expression. The *in situ* hybridization of RNAi treated embryos using the *Bm-wnt1* probe indicated that the target gene expression was markedly reduced, suggesting that the RNAi was effective (Supplementary Fig. 3). A previously study reported that *Bm-wnt1* knockdown resulted in severely truncated embryos (Yamaguchi et al., 2011). Similar truncated embryos were observed in the RNAi experiment in the present study (n=26/26). However, the phenotypes appeared to be more severe than those previously reported. *Bm-wnt1*RNAi embryos in this study comprised head with some epidermal structures attached. In these embryos, appendages other than the labrum and antenna were not clearly identifiable: thoracic legs were not observed, which contrasted with to the existence of immature three thoracic legs in the previous study (Fig. 5, Supplementary Fig. 5, Yamaguchi et al., 2011). *Bm-ovo* RNAi expression was then compared between wild type and RNAi-treated embryos fixed at about 26h AEL. In RNAi treated embryos, changes in *Bm-ovo* expression pattern were observed. While stripes that were clearly visible in the middle part of wild type embryos were absent in RNAi treated embryos, weak expression was noted from middle to the posterior. However, expression in anterior and posterior body region remained in treated embryos (n=19/19; Fig. 4E, F).

Discussion

Implications of the ovo homolog in Bombyx segmentation

This study revealed embryonic *Bm-ovo* expression patterns and some functions. *Bm-ovo* was dynamically expressed along the AP axis in a manner that resembled gap and pair-rule genes, and RNAi-treated embryos showed anomalies in anterior and posterior body parts, together with alterations in pair-rule gene expression patterns. The expression pattern and results of a molecular analysis of RNAi appeared to be roughly consistent with the morphological changes observed in *Bm-ovo* RNAi embryos. Assuming that, as a rough estimate, *Bm-eve* stripe #3 coincides with the posterior mesothoracic (T2) segment and the *Bm-eve* stripe # 2 posterior labium and *Bm-run* and *Bm-odd* stripe #2 exist in between, the weak expression of *Bm-eve* stripe #2 and #3 and *Bm-run* and *Bm-odd* stripe #2 may lead to aberrant gnathal/thoracic morphologies. For the observed posterior phenotypes, only the strongly expressed *Bm-ovo* domain appeared to be responsible. If this is the case, the abdominal phenotypes may be interpreted as the correct formation of the A1 to A5 segments with fused subsequent segments, and the region corresponding to the expression of *Bm-eve* stripe #7 contributes to the formation of the seventh abdominal segment because *Bm-eve* stripes#6 and #8, which strongly expressed the *Bm-ovo* domain cover, are expected to be mainly expressed in the posterior parts of A5 and A7, respectively.

Therefore, it is reasonable to assume that the changes observed in the expression of pair-rule genes are responsible for the observed morphological consequences. However, the mechanisms that cause these phenotypes appear to differ between the anterior and posterior regions because while the posterior phenotype was caused by deficiencies in pair-rule patterning, the pair-rule gene expression pattern in the anterior suggested that the pair-rule patterning itself is normal. The weak expression of the specific stripes of pair-rule genes is likely to be a secondary effect, i.e., caused by some mechanisms after normal patterning is achieved, such as an effect on mRNA stability.

On the other hand, given the broad expression along the AP axis of *Bm-ovo*, the observed phenotypes appeared to be modest; anomalies in the head or anterior abdominal segments, corresponding to strong head and weak expression around *Bm-eve* stripe #4 or #5, may be expected. The failure to detect corresponding phenotypes may reflect inefficiency in RNAi or the presence of redundant systems masking their manifestations.

Regulation of Bm-ovo expression

Although some irregularities were observed in segmental *Bm-wnt1* stripes in *Bm-ovo* RNAi embryos, no difference was noted from wild type embryos in the posterior expression domain. Since *Bm-ovo* influences pair-rule gene expression as described above, the irregular stripe phenotype may be mediated through its effects on pair-rule gene functions. However, *Bm-ovo* does not appear to influence posterior organizing function of *Bm-wnt1*. On the other hand, *Bm-wnt1* RNAi resulted in a change in *Bm-ovo* patterning. These results suggest that the regulation of *Bm-ovo* is controlled by the posterior organizing function of *Bm-wnt1*, appears to be complex, and may also be under the control of signaling pathways other than that of *Bm-wnt1* because *Bm-wnt1* RNAi did not result in a simple reduction in the expression of *Bm-ovo*. In *Drosophila* epidermal patterning system, *ovo*/*svb* receive inputs from Egfr pathway as well as Wingless signaling, albeit indirectly. Moreover, with its more immediate regulators, SoxN and Dichaete, *ovo*/*svb* has feedback relationships. It currently remains unclear whether similar regulatory events are operating in *Bombyx* segmentation process. However, changes in the patterning observed in *Bm-ovo* expression suggests a similarity in the system operating in *Bombyx* with those of *Drosophila* epidermal patterning, in which Wg represses *ovo*/*svb* expression and contributes to spatially restricting the *ovo*/*svb* expression domain. *Drosophila wg* is a segment polarity gene that is not involved in early segmentation events observed in short germ insects and in *Bombyx*. The involvement of Wg pathway in early segmentation appears to represent an ancestral condition. On the other hand, *Dichaete* is involved in *Drosophila* segmentation, with a dynamic expression pattern reminiscent of gap and pair-rule genes as in the case of *Bm-ovo* (Nambu and Nambu, 1996; Russell et al., 1996). The role of *Dichaete* in *Drosophila* segmentation may be an evolutionary remnant of the ancestral Wg pathway, possibly involving an *ovo* homolog. In this perspective, it is interesting that preliminary results suggested that *Bombyx Dichaete* (*Bm-Dct*) is also involved in segmentation (Supplementary Fig. 6).

Information obtained in *Drosophila* or other systems suggests the involvement of *ovo* homologs in cell differentiation and maintenance. More recently, a study of a human homolog of *ovo* indicated that it may act as a switch to enable the initiation of differentiation from the progenitor cell state by repressing stem-like properties (Renaud

et al., 2015). The involvement of *Bm-ovo* in *Bombyx* segmentation suggests the existence of a critical step common to transition from an undifferentiated to differentiated state or a cell fate decision process in ancient insect segmentation mechanisms, which is under control of *wnt* homologs.

References

Beermann, A., Prühs, R., Lutz, R. and Schröder, R. (2011) A context-dependent combination of Wnt receptors controls axis elongation and leg development in a short germ insect. *Development* 138: 2793-2805.

Bolognesi, R., Farzana, L., Fischer, T. D. and Brown, S. J. (2008). Multiple Wnt genes are required for segmentation in the short-germ embryo of *Tribolium castaneum*. *Curr. Biol.* 18: 1624-1629.

Bolognesi, R., Fischer, T. D. and Brown, S. J. (2009). Loss of *Tc-arrow* and canonical Wnt signaling alters posterior morphology and pair-rule gene expression in the short-germ insect, Tribolium castaneum. *Dev. Genes Evol*. 219: 369-375.

Cerny, A., Bucher, G., Schröder, R. and Klingler, M. (2005). Breakdown of abdominal patterning in the *Tribolium Krüppel* mutant *jaws*. *Development* **132**, 5353-5363.

Choe, C. P., Miller, S. C. and Brown, S. J. (2006). A pair-rule gene circuit defines segments sequentially in the short-germ insect *Tribolium castaneum*. *Proc. Natl. Acad. Sci. USA* **103**, 6560-6564.

Dai, X., Sconbaum, C., Degenstein, L., Bai, W., Mahowald, A. and Fuchs, E. (1998) The *ovo* gene required for cuticle formation and oogenesis in flies is involved in hair formation and spermatogenesis in mice. *Genes Dev*. 12 (21): 3452-3463.

Davis, G.K. and Patel, N.H. (2002). Short, long, and beyond: molecular and embryological approaches to insect segmentation. *Annu. Rev. Entomol.* **47**, 669-699.

El-Sherif, E., Averof, M. and Brown, S. J. (2012). A segmentation clock operating in blastoderm and germband stages of *Tribolium* development. *Development* **139**, 4341-4346.

Johnson, A. D., Fitzsimmons, D., Hagman, J. and Chamberlin. (2001) EGL-38 Pax regulates the ovo-related gene lin-48 during Caenorhabditis elegans organ development. Development 128, 2857-2865.

Liu, P.Z., Kaufman, T.C. (2004) *Krüppel* is a gap gene in the intermediate germband insect *Oncopeltus fasciatus* and is required for development of both blastoderm and germband-derived segments. Development 131, 4567–4579.

Liu, P. Z. and Kaufman, T.C. (2005) Short and long germ segmentation: unanswered questions in the evolution of a developmental mode. *Evol. Dev.* **7: 6**, 629-646.

Lynch, J.A., El-Sherif, E., Brown, S.J. (2012) Comparisons of the embryonic development of *Drosophila*, *Nasonia*, and *Tribolium*. WIREs Dev. Biol. 1, 16-39.

Mito, T., Okamoto, H., Shinahara, W., Shinmyo, Y., Miyawaki, K., Ohuchi, H. and Noji, S. (2006) *Krüppel* acts as a gap gene regulating expression of *hunchback* and *even-skipped* in the intermediate germ cricket *Gryllus bimaculatus*. *Dev. Biol.* **294**, 471-481.

Mita, K., Kasahara, M., Sasaki, S., Nagayasu, Y., Yamada, T., Kanamori, H., Namiki, N., Kitagawa, M., Yamashita, H., Yasukochi, Y., Kadono-Okuda, K., Yamamoto, K., Ajimura, M., Ravikumar, G., Shimomura, M., Nagamura, Y., Shin-I, T., Abe, H., Shimada, T., Morishita, S. and Sasaki, T. (2004). The genome sequence of silkworm, *Bombyx mori*. *DNA Res.* **11(1)**, 27-35.

Mita, K., Morimyo, M., Okano, K., Koike, Y., Nohata, J., Kawasaki, H., Kadono-Okuda, K., Yamamoto, K., Suzuki, M. G., Shimada, T., Goldsmith, M. R. and Maeda, S. (2003) The construction of an EST database for Bombyx mori and its application. *Proc. Natl. Acad. Sci. USA* 100 (24): 14121-12146.

Miyawaki, K., Mito, T., Sarashina, I., Zhang, H., Shinmyo, Y., Ohuchi, H. and Noji, S. (2004). Involvement of Wingless/Armadillo signaling in the posterior sequential segmentation in the cricket, *Gryllus bimaculatus* (Orthoptera), as revealed by RNAi analysis. *Mech. Dev*. 121: 119-130.

Myohara, M. (1994). Fate mapping of the silkworm, *Bombyx mori*, using localized irradiation of the egg at fertilization. *Development* **120**, 2869-2877.

Nagy, L., Riddiford, L. and Kiguchi, K. (1994). Morphogenesis in the early embryo of the Lepidopteran *Bombyx mori*. *Dev. Biol*. **165**, 137-151.

Nakao, H. (1999). Isolation and characterization of a *Bombyx vasa*-like gene. *Dev. Genes Evol.* **209**, 312-316.

Nakao, H., Matsumoto, T., Oba, Y., Niimi, T. and Yaginuma, T. (2008). Germ cell specification and early embryonic patterning in *Bombyx mori* as revealed by *nanos* orthologues. *Evol. Dev.* **10:5**, 546-554.

Nakao, H. (2010). Characterization of *Bombyx* embryo segmentation process: Expression profiles of *engrailed*, *even skipped*, *caudal* and *wnt1*/*wingless* homologues. *J. Exp. Zool. PartB Mol. Dev. Evol.* **314B**, 224-231.

Nakao, H. (2012). Anterior and posterior centers jointly regulate *Bombyx* embryo body segmentation. *Dev. Biol*. **371**, 293–301.

Nakao, H. (2015). Analyses of interactions among pair-rule genes and the gap gene *Krüppel* in *Bombyx* segmentation. *Dev. Biol.* **371**, 293–301.

Nakao, H. (2016). Hunchback knockdown induces supernumerary segment formation in Bombyx. *Dev. Biol.* **413**, 207-216

Nambu, P. A. and Nambu, J. R. (1996) The Drosophila fishhook gene encodes a HMG domain protein essential for segmentation and CNS development. Development 122, 3467-3475.

Oliver, B., Perrimon, N. and Mahowald, A. P. (1987) The *ovo* locus is required for sex-specific germ line maintenance in *Drosophila*. *Genes Dev*. 1: 913-923.

Overton, P. M., Chia, W. and Buescher, M. (2007) The *Drosophila* HMG-domain proteins SoxNeuro and Dichaete direct trichome formation via the activation of *shavenbaby* and the restriction of Wingless pathway activity. *Development* 134 (15): 2807-2813.

Pankratz, M. J. and Jäckle, H. (1993). Blastoderm segmentation. In *The development of Drosophila melanogaster* (ed. M. Bate and A. M. Arias), pp. 467-516. New York: Cold Spring Harbor Laboratory Press.

Peel, A.D., Chipman, A.D. and Akam, M. (2005). Arthropod segmentation: Beyond the *Drosophila* paradigm. *Nature Rev. Genet*. **6**, 905-916.

Renaud, S. J., Chakraborty, D., Mason, C. W., Karim Rumi, M. A., Vivian, J. L. and Soares, M. J. (2015) OVO-like 1 regulates progenitor cell fate in human trophoblast development. *Proc. Natl. Acad. Sci. USA* 112 (45): E61275-E6184.

Russell, S. R. H., Sanchez-Soriano, N., Wright, C. R. and Ashburner, M. (1996) The Dichaete gene of Drosophila melanogaster encodes a SOX-domain protein required for embryonic segmentation. Development 122, 3669-3676.

Rosenberg, M.I., Brent, A. E., Payre, F. and Desplan, C. (2014). Dual mode of embryonic development is highlighted by expression and function of *Nasonia* pair-rule genes. *eLife* **3**: e01440.

Sarrazin, A. F., Peel, A. D. and Averof, M. (2012). A segmentation clock with two-segment periodicity in insects. *Science* **336**, 338-341.

Wieschaus, E., Nüsslein-Volhard, C. and Jürgens, G. (1984) Mutations affecting the pattern of the larval cuticle in *Drosophila melanogaster*. Part III. Aygotic loci on the X-chromosome and fourth chromosome. *Roux Arch. Dev. Biol*. 193: 296-307.

Xue, R., Hu, X., Cao, G., Huang, M., Xue, G., Qian, Y., Song, Z. and Gong, C. (2014) Bmovo-1regulates ovary size in the silkworm, Bombyx mori. *PLoS One* 9(8): e10492B.

Yamaguchi, J., Mizoguchi, T. and Fujiwara, H. (2011) siRNAs induce efficient RNAi response in *Bombyx mori* embryos. *PLoS One* **6***,* e25469*.*

Yatsu, J., Hayashi, M., Mukai, M., Arita, K., Shigenobu, S. and Kobayashi, S. (2008) Maternal RNAs encoding transcription factors for germline-specific gene expression in *Drosophila* embryos. *Int. J. Dev. Biol.* **52**, 913-923.

Figure Legends

Figure 1. *Bm-ovo* expression at early embryonic stages. Embryos were fixed at the indicated AEL times and stained with the *Bm-ovo* probe (A, C, D, F, H and I; blue) or double stained together with the *Bm-eve* probe (E, G; *Bm-ovo*: red, *Bm-eve*: blue). (B) Propidium Iodide (PI) image of A. Nuclei were not observed at this stage as shown. The anterior is to the left. (A-C) Ventral view. (D-I) Lateral view. (D-G) The ventral side is up. (H-I) The dorsal side is up. Digits indicate *Bm-eve* stripe numbers. Two weakly expressed bands are in brackets. The *Bm-ovoCp* probe was used in this experiment.

Figure 2. Morphologies of *Bm-ovo* RNAi embryos at 72 hours AEL. Wild-type (A) or *Bm-ovo* RNAi-treated embryos (B, C) were fixed at 72 hours AEL and stained with PI. Lateral view. The anterior is to the left. The dorsal side is up. Asterisks indicate prolegs. Wild-type embryos possess four proleg-bearing segments (A), whereas *Bm-ovo* RNAi-treated embryos have three (B). Note that in RNAi-treated embryos, the posterior abdominal segments and dorsal side of the meso- (T2) and meta-thoracic (T3) segments were fused (B). The dorsally fused T2 and T3 segments are in brackets. In C, irregularly shaped segments were observed (arrows). at: antenna. md: mandible. mx: maxilla. li:

labium. T1: prothorax. T2: mesothorax. T3: metathorax. A6~A9: sixth, seventh, eighth, and ninth abdominal segments, respectively.

Figure 3. Pair-rule gene expression was altered in *Bm-ovo* RNAi-treated embryos. Wild-type (A, C, E) or *Bm-ovo* RNA-treated embryos (B, D, F) were fixed at approximately 25-27 hours AEL and subjected to *in situ* hybridization in order to examine pair-rule gene expression patterns: (A, B) *Bm-eve*, (C, D) *Bm-run* and (E, F) *Bm-odd*. Lateral view. The anterior is to the left. The ventral side is up. Digits indicate the stripe number of the indicated pair-rule genes. See the text for details. The *Bm-ovoCp* probe was used in this experiment.

Figure 4. Interactions between *Bm-ovo* and *Bm-wnt1*. (A-D) Wild type and *Bm-ovo* RNAi treated embryos were fixed (A, B: at 23h AEL, C, D: at 26h AEL) and stained for *Bm-wnt1*. (E, F) Wild type and *Bm-wnt1* treated embryos were fixed at 26h AEL and stained for *Bm-ovo*. Lateral view. The anterior is to the left. The ventral side is up. The arrow in (F) indicates the anterior boundary of the middle expression domain. See the text for details. The *Bm-ovoCp* probe was used in this experiment.

Figure 5. Morphologies of wild type (A) and *Bm-wnt1*RNAi treated (B) embryos. Embryos were fixed after blastokinesis (~5d AEL) and stained with PI. Lateral view. at: antenna. lr: labrum. md: mandible

Acknowledgment

I thank the anonymous reviewers and Editor for their valuable comments and suggestions. I also thank Dr. Kakeru Yokoi at NARO for his assistance.

Table 1. Summary of *Bmovo* RNAi embryo phenotypes using different dsRNA.

		Observed phenotype frequency (number of observed/total embryos)			
		Defects in gnathal/thoracic segments	number of abdominal segments		
			6	7	8
dsRNA used	Bm-ovoC RNAi	5/14	1/14	10/14	3/14
	Bm-ovoE1RNAi	18/19	17/19	2/19	0/19
	Bm-ovoE3-4RNAi	11/22	16/22	6/22	0/22

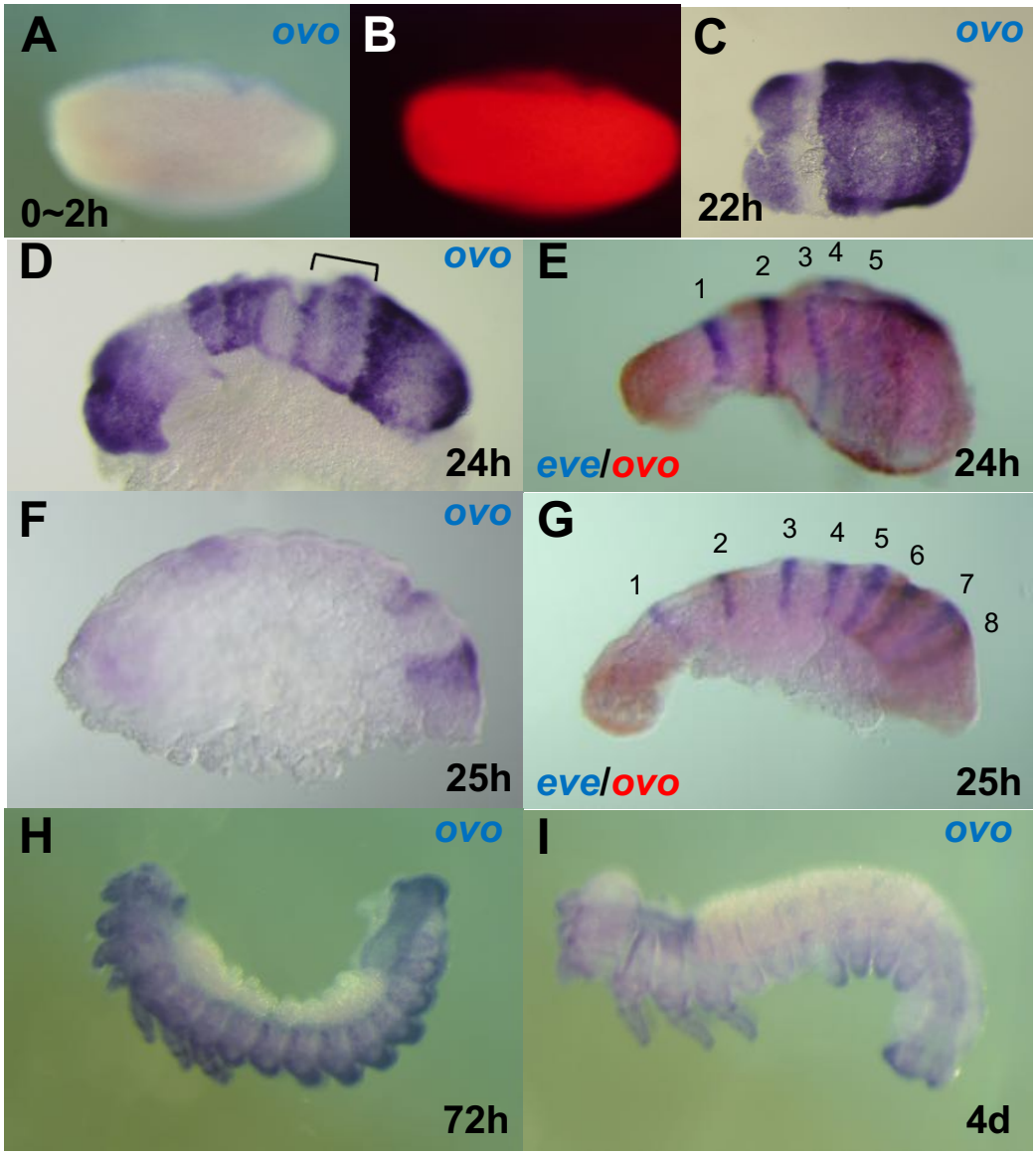
A
ovo
0~2h
B
C
ovo
22h
D
ovo
24h
E
1
2
3
4
5
eve/ovo
24h
F
ovo
25h
G
1
2
3
4
5
6
7
8
eve/ovo
25h
H
ovo
72h
I
ovo
4d

Figure 1

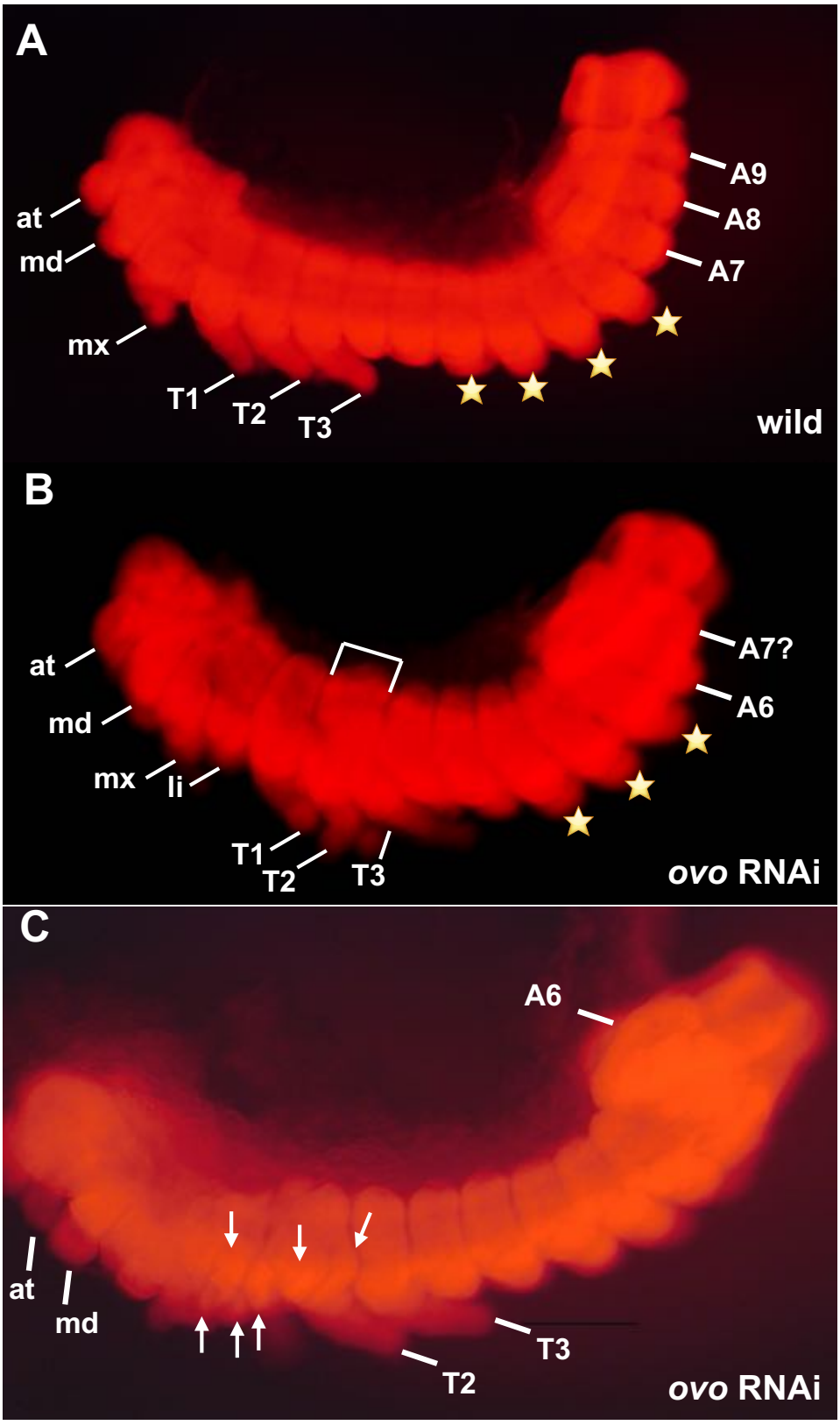
A
at
md
mx
T1
T2
T3
A9
A8
A7
wild
B
at
md
mx
li
T1
T2
T3
A7?
A6
ovo RNAi
C
A6
at
md
T2
T3
ovo RNAi

Figure 2

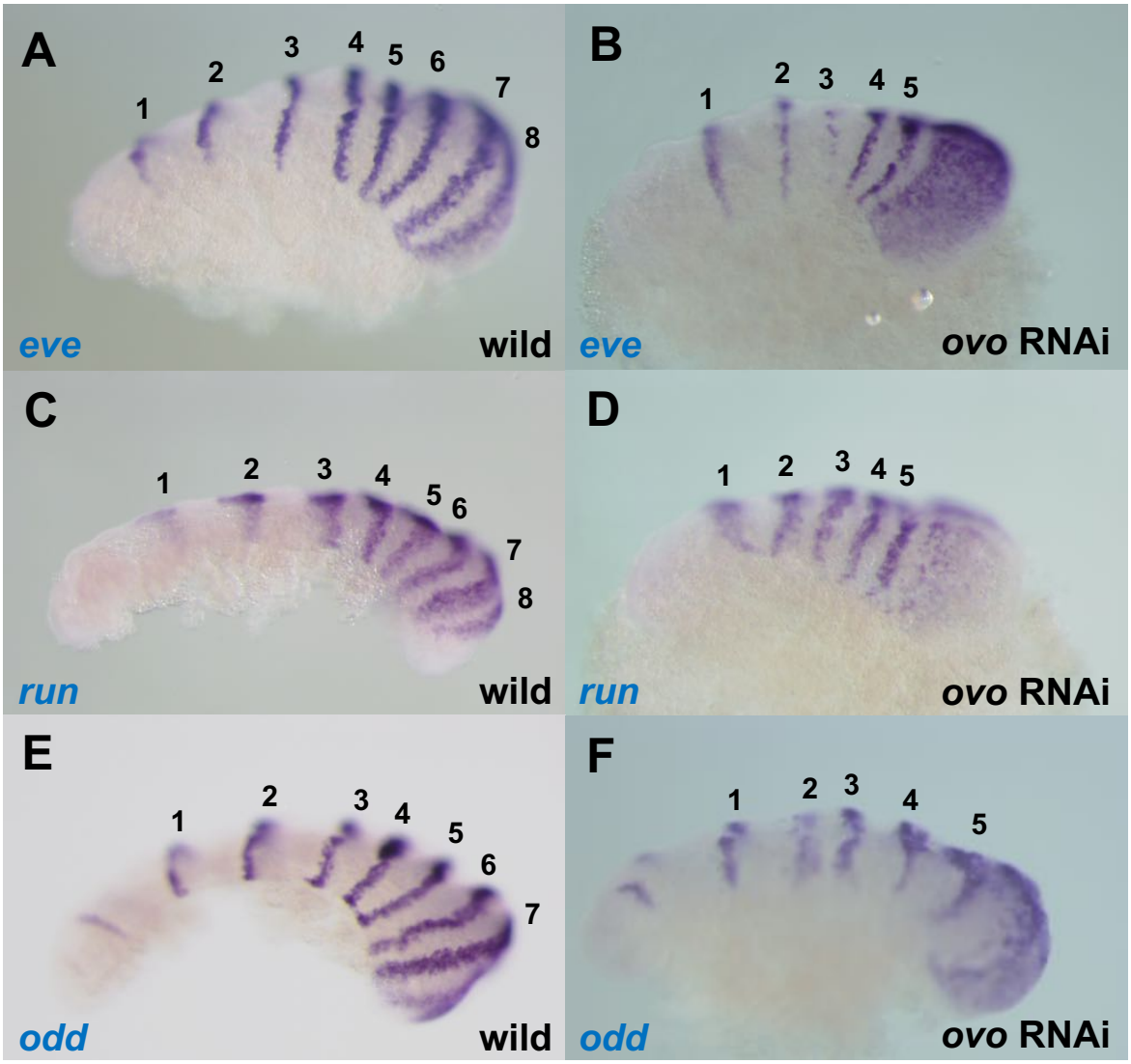
A
1
2
3
4
5
6
7
8
eve
wild
B
1
2
3
4
5
eve
ovo RNAi
C
1
2
3
4
5
6
7
8
run
wild
D
1
2
3
4
5
run
ovo RNAi
E
1
2
3
4
5
6
7
odd
wild
F
1
2
3
4
5
odd
ovo RNAi

Figure 3

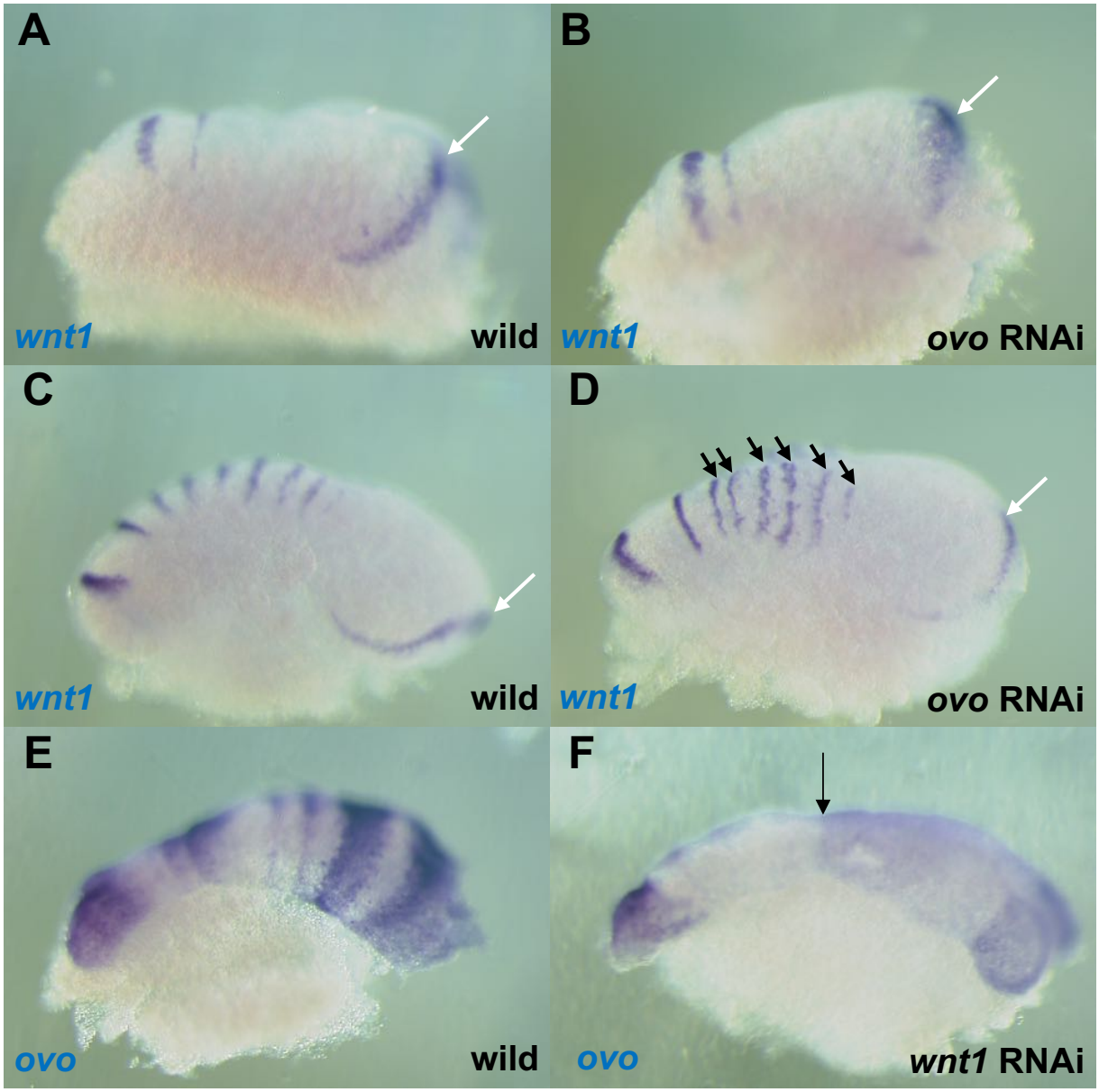
A
wnt1
wild
B
wnt1
ovo RNAi
C
wnt1
wild
D
wnt1
ovo RNAi
E
ovo
wild
F
ovo
wnt1 RNAi

Figure 4

Figure5

Supplementary Figure 1. An analysis of embryonically expressed *Bm-ovo* open reading frame (ORF) species. The PCR primer pair was prepared around DNA regions corresponding to the start and stop codons in order to amplify the full ORF, and amplification was performed using cDNAs prepared at the indicated AEL times. In both cases, a strong band of approximately 2.6 kbp was detected (arrow). Other weak bands were also faintly observed; however, their identities currently remain unknown.

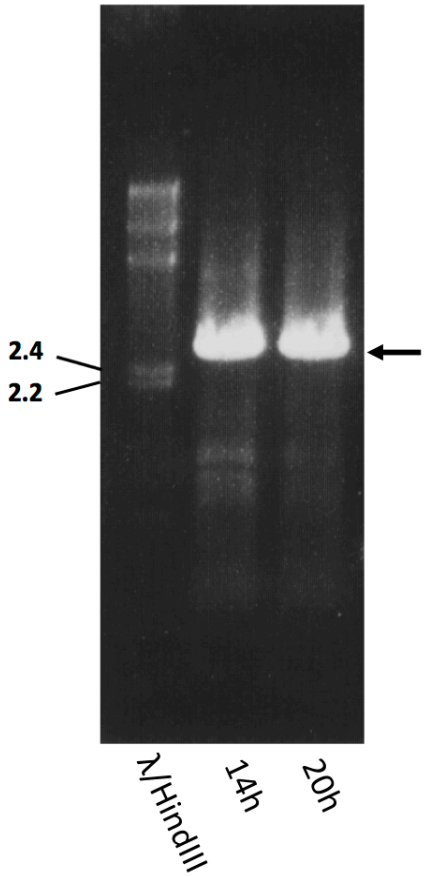

Supplementary Figure 2. *Bm-ovo* expression at 26h AEL stained with *Bm-ovo* probes corresponding to different regions of the *Bm-ovo* gene. Embryos were fixed and stained using the probes indicated. Lateral view. The anterior is to the left. The ventral side is up. Essentially the same staining pattern was observed for all the probes used. Scale bar: 0.2mm.

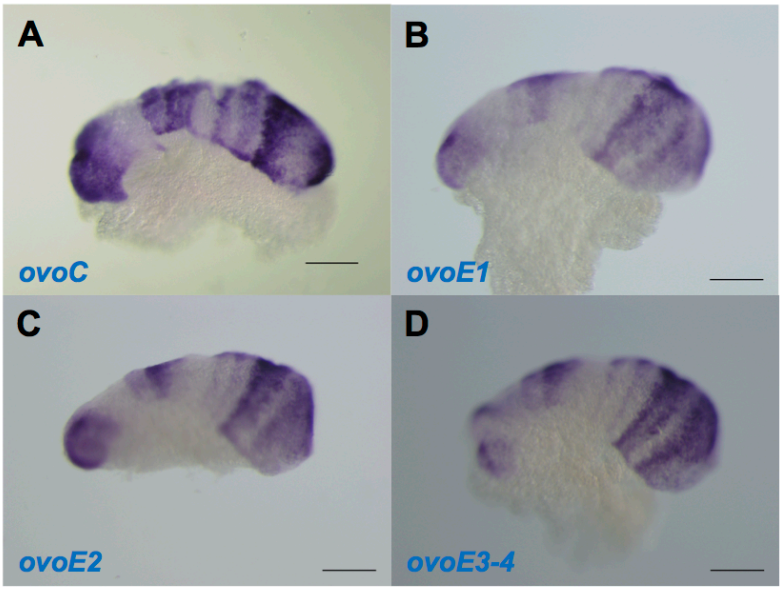

Supplementary Figure 3. *Bm-wnt1* RNAi and *Bm-ovo* RNAi were effective. Wild type, *Bm-wnt1*RNAi-, and *Bm-ovo*RNAi-treated embryos were fixed and stained with probes targeted by RNAi. (A-C) Wild type embryos (A) and embryos subjected to *Bmwnt1RNAi1*(B) and *Bmwnt1RNAi2* (C) were fixed at 26h AEL and stained with the *Bm-wnt1* probe. Wild type embryos (D) and embryos subjected to *BmovoCRNAi1*(E) were fixed at 26h AEL and stained with *Bm-ovoCp*. Wild type embryos (F) and embryos treated with *BmovoE1RNAi1*(G) and *BmovoE3-4RNAi2* (H) were fixed at 23h AEL and stained with *Bm-ovoE2p*. The anterior is to the left. (A-E) Lateral view. The ventral side is up (F-H) Ventral view. Scale bar: 0.2mm. Dashed lines approximate the boundaries of germ bands.

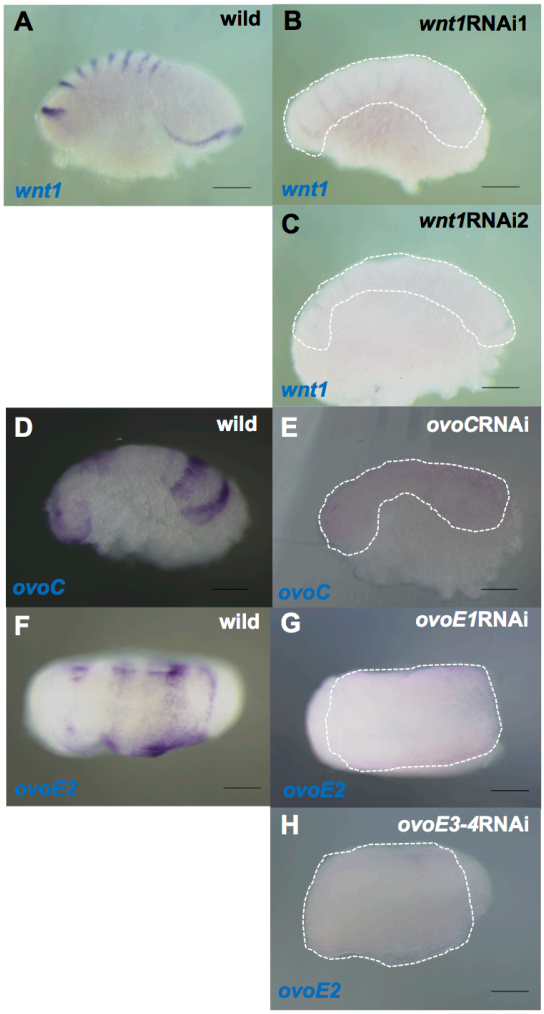

Supplementary Figure 4. An example of *Bm-ovo* RNAi treated embryos fixed at 23h AEL and stained for *Bm-run*. The anterior is to the left. Lateral view. The ventral side is up. Note that the intensity of #2 stripe is weaker than those of the other stripes (stripes #1, 3 and 4).

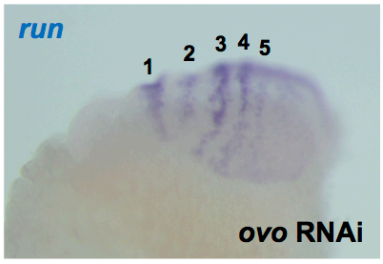

Supplementary Figure 5. Examples of mature *Bm-wnt1* RNAi treated embryos. (A) A comparison of the morphologies of a wild type (left) and *Bm-wnt1* RNAi embryo (right). In *Bm-wnt1* RNAi-treated embryos, incomplete head capsules with some epidermal structure attached posteriorly was observed. (B, B') An example of an RNAi treated embryo. Dorsal or ventral views are shown, respectively. (C, C') show another example. The anterior is to the left. As shown, gnathal appendage structures were not observed in *Bm-wnt1* treated embryos and thoracic legs were absent. Arrows indicate head capsules. Scale bar in A indicates 0.5mm.

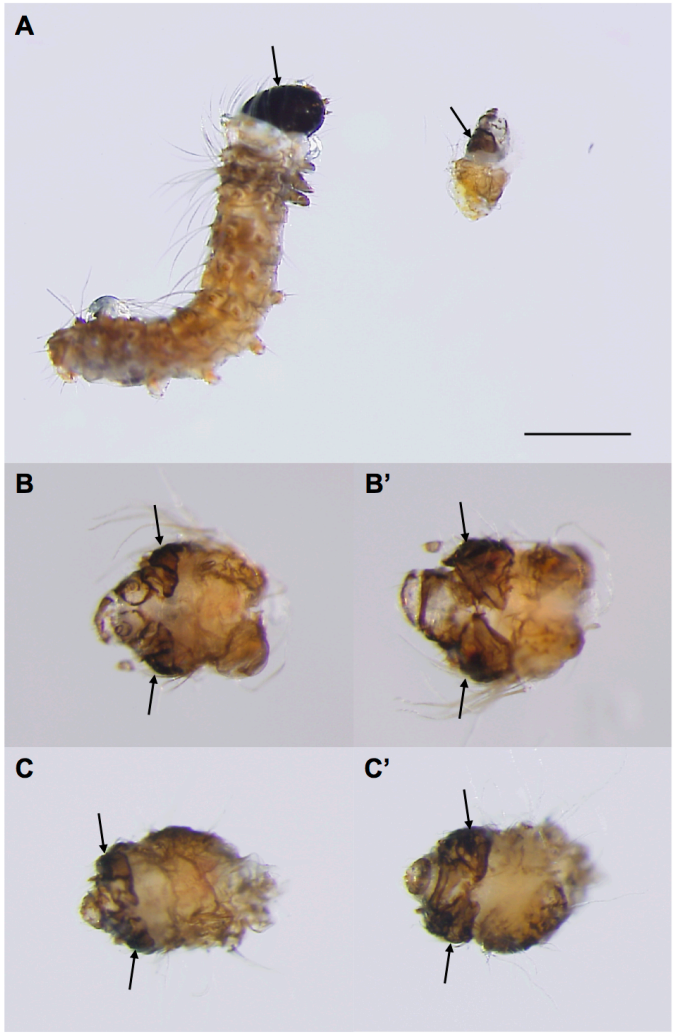

Information on *Bombyx Dichaete* (*Bm-Dct*) has been deposited in KAIKObase (gene ID: BMgn003079). Based on sequence information, dsRNA targeting at *Bm-Dct* was prepared as described in the **Materials and Methods** section and subjected to an RNAi analysis. The sequences of the primers used for the amplification of the dsRNA template were: 5'-TAATACGACTCACTATAGGGAGATGTCGACTTTGAGCCATCAC-3', 5'-TAATACGACTCACTATAGGGAGAGGTGCCATTAGCTTGGAGAA-3'.

Supplementary Figure 6. Morphology of a *Bm-Dct* RNAi-treated embryo. Wild-type (A) or *Bm-Dct* RNAi-treated (B) embryos were fixed at 72 hours AEL and stained with PI. Although some normal morphogenesis appears to occur in the head region in the *Bm-Dct* RNAi-treated embryo, the trunk region is aberrant (n=20/20). lr: labrum. at: antenna. md: mandible. mx: maxilla. li: labium. T1: prothorax. T2: mesothorax. T3: metathorax. Arrows indicate appendages of unknown identities.